The Insulin-like Growth Factor-1 Receptor–Targeting Antibody, CP-751,871, Suppresses Tumor-Derived VEGF and Synergizes with Rapamycin in Models of Childhood Sarcoma

Raushan T. Kurmasheva,[1] Lorina Dudkin,[1] Catherine Billups,[2] Larisa V. Debelenko,[3] Christopher L. Morton,[1] and Peter J. Houghton[1]

Departments of [1]Molecular Pharmacology, [2]Biostatistics, and [3]Pathology, St. Jude Children's Research Hospital, Memphis, Tennessee

Abstract

Signaling through the type 1 insulin-like growth factor receptor (IGF-1R) occurs in many human cancers, including childhood sarcomas. As a consequence, targeting the IGF-1R has become a focus for cancer drug development. We examined the antitumor activity of CP-751,871, a human antibody that blocks IGF-1R ligand binding, alone and in combination with rapamycin against sarcoma cell lines *in vitro* and xenograft models *in vivo*. In Ewing sarcoma (EWS) cell lines, CP751,871 inhibited growth poorly (<50%), but prevented rapamycin-induced hyperphosphorylation of AKT(Ser473) and induced greater than additive apoptosis. Rapamycin treatment also increased secretion of IGF-1 resulting in phosphorylation of IGF-1R (Tyr1131) that was blocked by CP751,871. *In vivo* CP-751,871, rapamycin, or the combination were evaluated against EWS, osteosarcoma, and rhabdomyosarcoma xenografts. CP751871 induced significant growth inhibition [EFS(T/C) >2] in four models. Rapamycin induced significant growth inhibition [EFS(T/C) >2] in nine models. Although neither agent given alone caused tumor regressions, in combination, these agents had greater than additive activity against 5 of 13 xenografts and induced complete remissions in one model each of rhabdomyosarcoma and EWS, and in three of four osteosarcoma models. CP751,871 caused complete IGF-1R down-regulation, suppression of AKT phosphorylation, and dramatically suppressed tumor-derived vascular endothelial growth factor (VEGF) in some sarcoma xenografts. Rapamycin treatment did not markedly suppress VEGF in tumors and synergized only in tumor lines where VEGF was dramatically inhibited by CP751,871. These data suggest a model in which blockade of IGF-1R suppresses tumor-derived VEGF to a level where rapamycin can effectively suppress the response in vascular endothelial cells. [Cancer Res 2009;69(19):7662–71]

Introduction

Deregulated insulin-like growth factor signaling through the type-1 receptor (IGF-1R) appears common to many childhood solid tumors and offers an important molecular target for developmental therapeutics. For example, the alveolar subtype of rhabdomyosarcoma (RMS) is associated with increased IGF-1R (1). For the embryonal RMS, the loss of imprinting at the IGF-2 locus may be a primary genetic event for embryonal RMS (2, 3). IGF-1R is a potent mediator of autocrine growth in Ewing sarcoma (EWS; refs. 4, 5), and EWS-FLI1 silencing leads to increased levels of insulin-like growth factor binding protein 3 gene, a major regulator of IGF-1 (6). Additionally, IGF-1 is a mitogen for osteosarcoma (OS; refs. 7–9), neuroblastoma (10, 11), brain tumors [including glioblastoma (12, 13), astrocytoma (14), and medulloblastoma (15)], Wilms tumor (16), and hepatocellular carcinoma (17).

IGF-1R has become a major focus for cancer therapeutics development with at least five fully human antibodies in adult phase I to III clinical trials (18–24). These agents show specificity for the IGF-1R, although they may also inhibit chimeric receptors formed through heterodimerization with the insulin receptor. In preclinical cancer models, antibody-mediated down-regulation of IGF-1R significantly retards growth of many tumors (25) and induces regressions when combined with cytotoxic agents (19, 26). These results are consistent with the significant literature that implicates IGF-1 signaling in survival of cells exposed to different cellular stresses (22).

The macrocyclic lactone antibiotic, rapamycin (sirolimus), is a highly specific inhibitor of mammalian target of rapamycin (mTOR), a conserved serine/threonine kinase. The role of mTOR Complex 1 (mTORC1) in tumorigenesis and survival has become apparent (27, 28). Rapamycin inhibits the proliferation of many tumor cell lines *in vitro* including cell lines derived from childhood cancers (29), and shows significant antitumor activity against syngeneic tumor models (30), and against childhood cancer xenografts (31). Rapamycin induced significant differences in event free survival (EFS) distribution in 33 of 44 (75%) solid pediatric tumor xenografts, showing particular activity against sarcoma and leukemia models (31).

We have tested the strategy of combining rapamycin with a human IGF-1 receptor–targeting antibody, CP-751,871, against cell lines and a comprehensive panel of more advanced stage xenograft models derived from childhood sarcomas. Rather surprisingly, our data show that in some sarcoma xenografts, IGF-1R significantly regulates the level of vascular endothelial growth factor (VEGF) and its transcription, whereas inhibition of mTORC1 has a minor effect on the level of VEGF in these sarcomas.

Materials and Methods

Cell lines and xenograft models. EWS cells and xenografts used in this study all express EWS/FLI1. The RMS cell lines and xenografts and OS

Note: Supplementary data for this article are available at Cancer Research Online (http://cancerres.aacrjournals.org/).

Current address for R.T. Kurmasheva, L. Dudkin, and P.J. Houghton: Childhood Cancer Center, Nationwide Children's Hospital, 700 Children's Drive, Columbus, OH 43205. E-mail: Peter.Houghton@nationwidechildrens.org.

Requests for reprints: Peter J. Houghton, Department of Molecular Pharmacology, St. Jude Children's Research Hospital, 332 North Lauderdale Street, Memphis, TN 38105. Phone: 901-595-3440; Fax: 901-595-4290; E-mail: peter.houghton@stjude.org.

©2009 American Association for Cancer Research.

doi:10.1158/0008-5472.CAN-09-1693

Downloaded from http://aacrjournals.org/cancerres/article-pdf/69/19/7662/2616060/7662.pdf by guest on 05 October 2022

xenografts have been described previously (32, 33). Cell lines were cultured in RPMI 1640 supplemented with 10% fetal bovine serum.

***In vitro* growth inhibition studies.** For prolonged serum-free experiments, EWS cells were cultured in modified N2E medium (34), and allowed to attach overnight. On the next day, 1 or 5 μg/mL of CP-751,871 was added to the fresh media. After 4 d of incubation, cell viability was assessed by Alamar Blue staining (Biosource).

Western blotting. Tumor tissue samples were pulverized under liquid N_2, and extracted as described previously (35). Immunoblotting procedures have been previously reported (35, 36). We used primary antibodies to β-actin (Santa Cruz Biotechnology), glyceraldehyde-3-phosphate dehydrogenase (GAPDH), ribosomal protein S6 (rpS6), phospho-rpS6 (Ser235/236), AKT, phospho-AKT(Ser473), IGF-1R, and pIGF-1R (Tyr1131, Cell Signaling). Immunoreactive bands were visualized by using SuperSignal Chemiluminiscence substrate (Pierce) and Biomax MR and XAR film (Eastman Kodak Co.).

ELISA assays. VEGF levels in culture were determined by ELISA as previously described (36). For determining IGFs and VEGFs in tumor tissue, tumor sample lysates were prepared from tumor tissue pulverized under liquid N_2. Protein (2 μg/mL) was used to run ELISA assay according to manufacturer's instructions (R&D Systems).

Quantitative real-time reverse transcription-PCR. Total RNA was extracted using TRI Reagent (Ambion) and purified to remove contaminating DNA (DNA free kit, Ambion). Total RNA (1 μg) was reverse transcribed with hexamer primers and M-MLV Reverse Transcriptase (Clontech). Gene expression of human VEGF and GAPDH was quantified on a Taqman 7900HT Thermal Cycler using Taqman Gene Expression Assays and Taqman Universal PCR Master Mix with no AmpErase UNG (Applied Biosystems). Real-time reverse transcription-PCR (RT-PCR) singleplex reactions, final volume of 50 μL per 3 μL cDNA were diluted in RNase-free water, 25 μL Universal Master Mix, and 2.5 μL of 20× Gene Expression Assay Mix. Amplification conditions were set up to 10 min at 95°C followed by 40 PCR cycles (15 s at 95°C, 1 min at 60°C). The quantity of cDNA used in each reaction was normalized to GAPDH and expressed as a ratio of sample cDNA to GAPDH cDNA.

Immunohistochemical studies. Tumor tissue was immediately fixed in formalin and processed using standard histologic procedures. Sections were stained with H&E and immunostained with mouse monoclocal Ki-67 antigen

Downloaded from http://aacrjournals.org/cancerres/article-pdf/69/19/7662/2616060/7662.pdf by guest on 05 October 2022

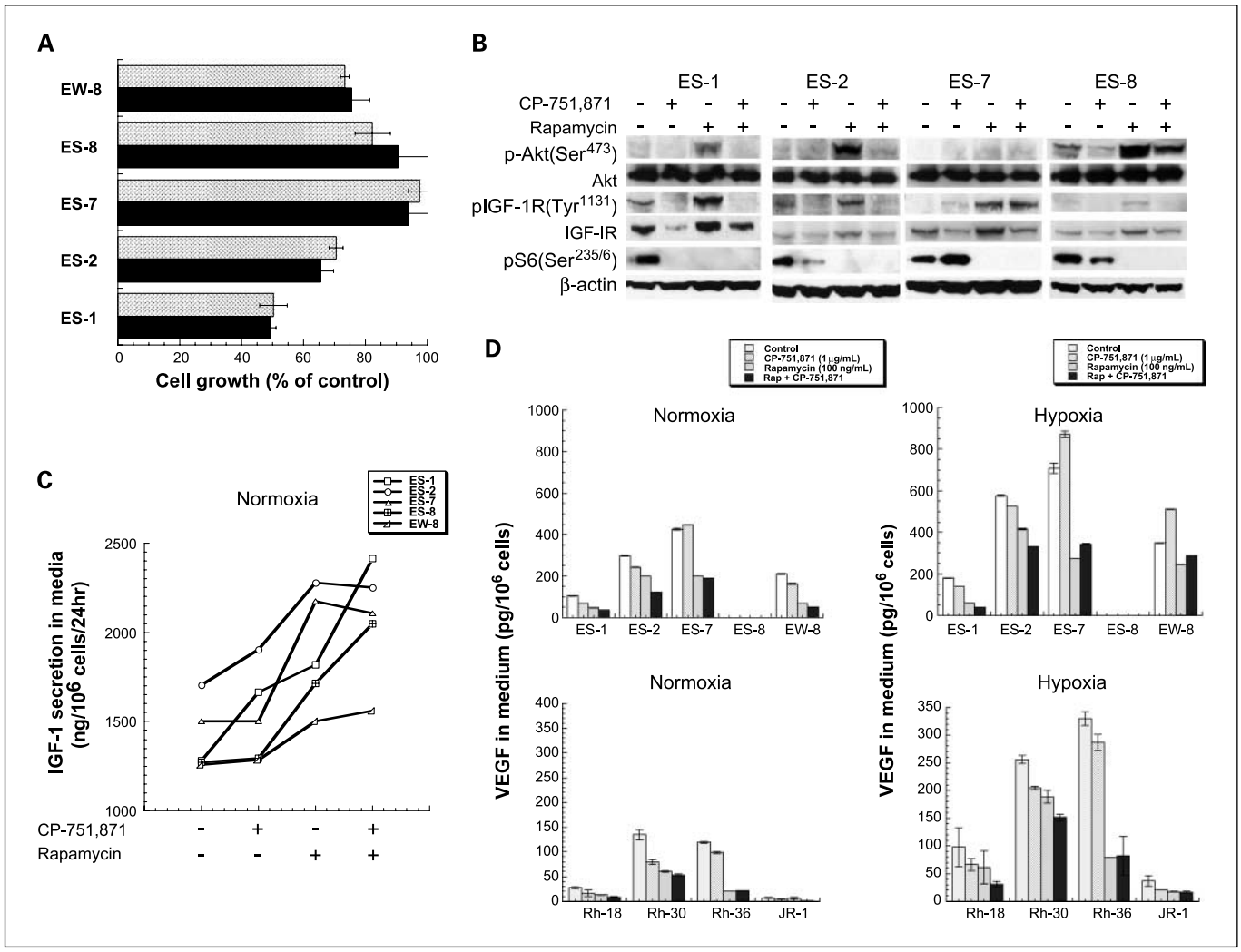

Figure 1. *In vitro* studies with CP-751,871. *A,* EWS cells were incubated in serum-containing medium ± CP-751,871 at 1 (*black columns*) or 5 μg/mL (*stippled columns*). Cell growth was determined by Alamar Blue staining after 4 d. Results are presented as percent control growth; *columns,* mean ($n = 3$); *bars,* SD. *B,* EWS cells were incubated with CP-751,871 (1 μg/mL), rapamycin (100 ng/mL), the combination, or without drugs for 24 h. Cell lysates were probed for total and phosphorylated IGF-1R, AKT, and S6. β-Actin serves as a loading control. *C,* EWS cells were incubated with CP-751,871 (1 μg/mL), rapamycin (100 ng/mL), the combination, or without drugs for 24 h. IGF-1 in media was determined by ELISA and expressed as ng/10^6 cells (mean, $n = 2$). *D,* EWS or RMS cells were grown under normoxic conditions (21% O_2) or hypoxic conditions (1% O_2) in the absence or presence of drugs. VEGF in media was determined by ELISA and expressed as pg/10^6 cells; *columns,* mean ($n = 3$); *bars,* SD.

antibody (clone MIB-1, DakoCytomation), following deparaffinization and antigen retrieval. Terminal deoxynucleotidyl transferase-mediated dUTP nick end labeling (TUNEL) assays were performed on the deparaffinized 4-μm sections using the Promega Dead End kit (ProMega).

***In vivo* tumor growth inhibition studies.** CB17SC-M *scid*$^{-/-}$ female mice (Taconic Farms) were used to propagate s.c. implanted sarcomas. All mice were maintained under barrier conditions and experiments were conducted using protocols and conditions approved by the institutional animal care and use committee. Tumor volumes (cm^3) and tumor responses were determined as previously described (see Supplemental response definitions; ref. 37).

Statistical methods. The exact log-rank test, as implemented using Proc StatXact for SAS, was used to compare EFS distributions between treatment and control groups and between combinations and respective single-agent treatment groups. *P* values were two sided and both unadjusted and Bonferroni-adjusted *P* values were presented for multiple comparisons.

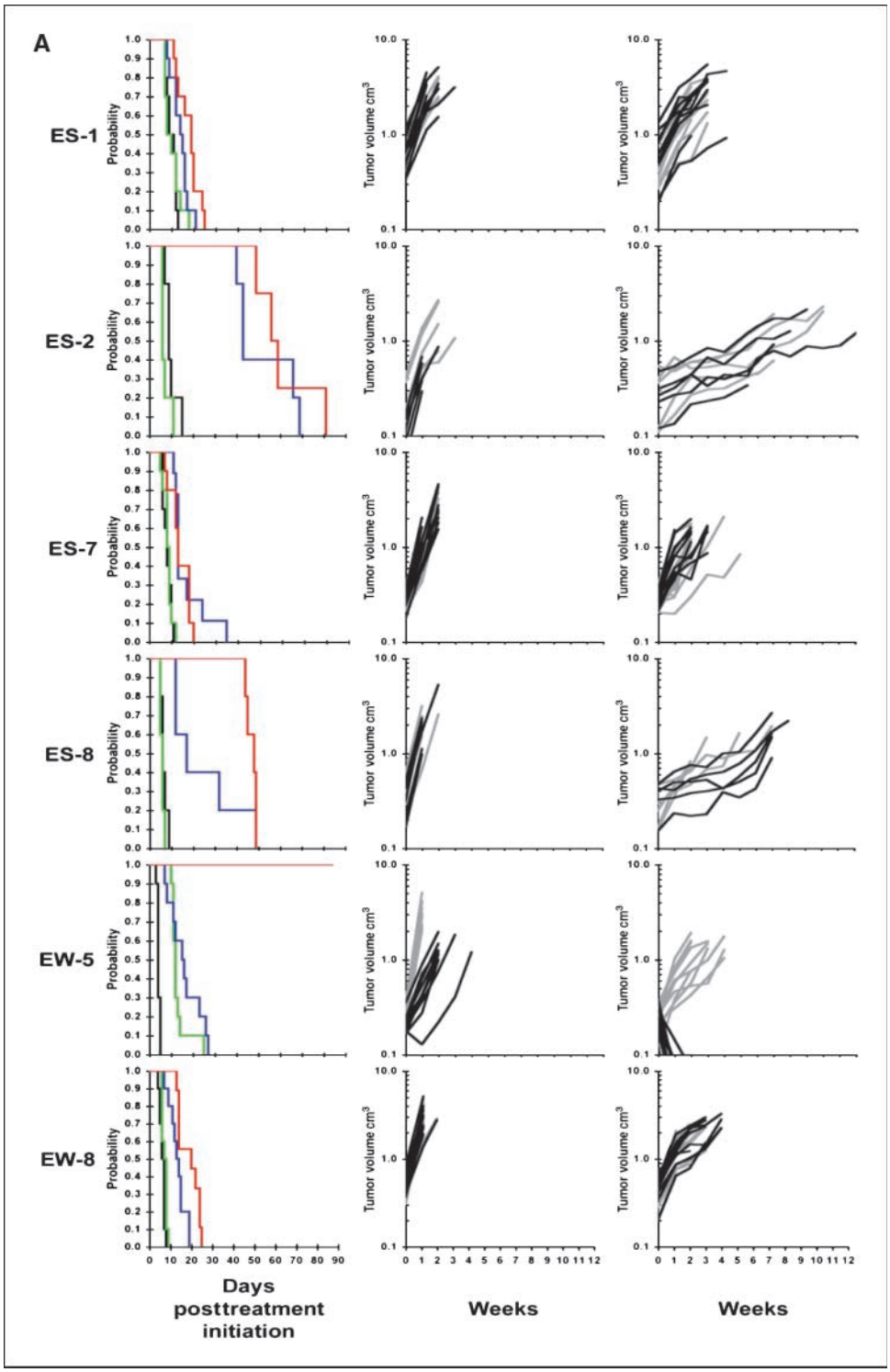

Figure 2. *A,* responses of EWS xenografts to CP-751,871, rapamycin, or the combination treatment.

Downloaded from http://aacrjournals.org/cancerres/article-pdf/69/19/7662/2616060/7662.pdf by guest on 05 October 2022

Drugs and formulation. Rapamycin was purchased from LC Laboratories, and CP-751,871 was generously provided by Bruce Cohen and James Christensen (Pfizer, Groton, CT and San Diego, CA). Mice received rapamycin (5 mg/kg) daily ×5 i.p. per week for up to 12 consecutive wk. CP-751,871 was administered by i.p. injection at 0.5 or 0.25 mg per mouse twice weekly for up to 4 wk.

Results

***In vitro* studies with EWS cells.** Maximum growth inhibition of EWS cell lines growing in serum-containing medium was achieved at 1 μg/mL CP-751,871, a monoclonal antibody that targets the human IGF-1R to prevent ligand binding (19). Maximum inhibition of growth was 50% (ES-1 cells), whereas under these growth conditions, ES-7 and ES-8 cell lines were essentially resistant to CP-751,871 (Fig. 1*A*). Previously, we reported that inhibition of mTORC1 signaling by rapamycin-induced apoptosis in sarcoma cells in serum-free medium (34). To determine whether concomitant inhibition of IGF-1R and mTORC1 signaling enhanced cell death compared with rapamycin alone, EWS cells were grown under serum-free conditions with or without rapamycin, CP-751,871, or with the combination of these agents. Apoptosis was determined by fluorescence-activated cell sorting analysis as previously described (34). CP-751,871 alone induced apoptosis in only ES-8 cells, whereas ~32% of EW-8 cells were determined to be apoptotic after 4 days of rapamycin treatment. Combined treatment with rapamycin and CP-751,871 was supra-additive in each EWS cell line examined, increasing the nonviable fraction in all cell lines tested (Supplementary Table S1).

Several studies have shown rapamycin-induced hyperphosphorylation of AKT (Ser473). The putative mechanism is through inhibition of S6K1, downstream of mTORC1, and relief of the negative feedback on IRS-1 (36, 38, 39). As shown in Fig. 1*B*,

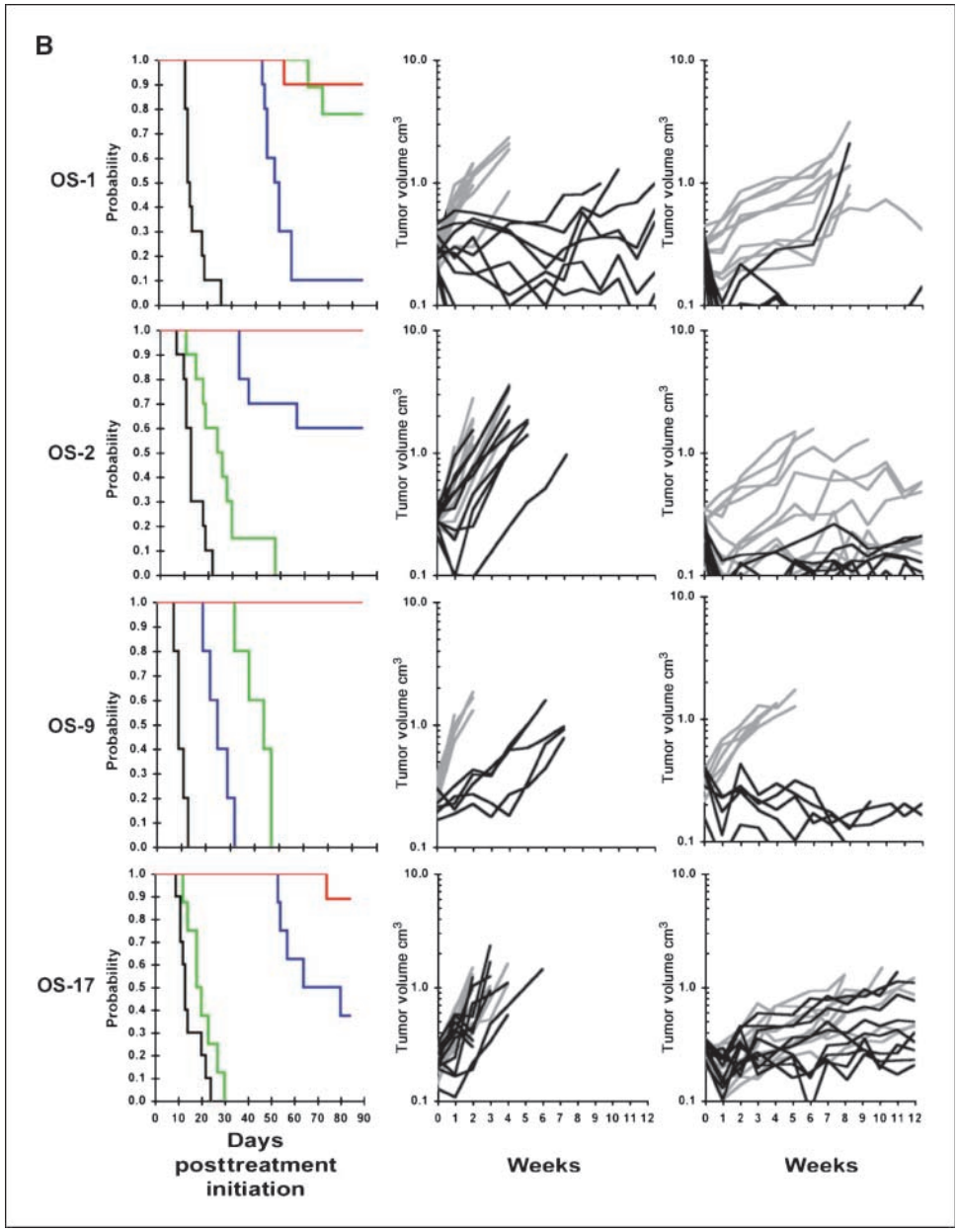

Figure 2 *Continued*. *B,* responses of OS xenografts to CP-751,871, rapamycin, or the combination treatment. Tumor-bearing mice were treated with CP-751,871 (0.25 mg/mouse twice weekly ×4). Rapamycin (5 mg/kg daily ×5 per week for up to 12 consecutive wk) or the combination of CP-751,871 and rapamycin. Tumor diameters were measured weekly. *Left,* Kaplan Meier EFS. *Black,* control; *green,* CP-751,871; *blue,* rapamycin; *red,* CP-751,871 + rapamycin. Curves show the probability of mice being event-free (tumor volume of <4-fold that at initiation of treatment) against days after treatment initiation. *Center,* growth of individual tumors; *light gray,* controls; *black,* CP-751,871 treated. *Right,* growth of individual tumors; *light gray,* rapamycin; *black,* CP-751,871 + rapamycin treated.

Downloaded from http://aacrjournals.org/cancerres/article-pdf/69/19/7662/2616060/7662.pdf by guest on 05 October 2022

rapamycin induced a robust increase in AKT(Ser473) phosphorylation in EWS cells and this was blocked by CP-751,871. Rapamycin also induced hyperphosphorylation of IGF-1R(Tyr1131), suggesting receptor activation by ligand. For all Ewing cell lines, rapamycin significantly increased IGF-1 secreted into the medium, suggesting that cells compensate for mTORC1 inhibition by inducing this survival factor (Fig. 1*C*). CP-751,871 alone increased IGF-1 in ES-1 and ES-2 cell lines only, whereas the combination of CP-751,871 with rapamycin was additive in ES-1, ES-8, and EW-8 lines.

Combined inhibition of IGF-1R and mTORC1 inhibits VEGF. Combined inhibition of AKT and mTORC1 synergistically suppresses VEGF secretion by RMS and neuroblastoma cells in culture (36). To determine whether simultaneous blockade of IGF-1R and mTORC1 could achieve similar effects on VEGF, cells were incubated for 24 hours under normoxia (21% O_2) or hypoxia (1% O_2) without or with CP-751,871, rapamycin, or both agents. At the end of the incubation period, medium was harvested and VEGF/10^6 cells were determined. As shown in Fig. 1*D* under normoxic conditions, the combination of inhibitors was essentially additive in reducing VEGF levels in most EWS and RMS cells, whereas CP-751,871 did not enhance the effect of rapamycin in reducing VEGF levels in ES-7 or Rh36 cells. Similar results were obtained under hypoxic conditions where the combination significantly reduced hypoxia-driven increases in levels of VEGF.

***In vivo* antitumor activity.** To determine whether this combination was therapeutically useful, we examined the antitumor activity of the individual agents and the combination of CP-751,871 with rapamycin in a series of xenograft models representing EWS (n = 6; Fig. 2*A*), OS (n = 4; Fig. 2*B*), and RMS (n = 2). A complete summary of results is shown in Supplementary Table S2. CP-751,871 was administered i.p. twice weekly for a planned 4 weeks only, whereas rapamycin was administered daily for 5 days per week for up to 12 consecutive weeks. CP-751,871 administered at 0.5 mg per mouse or 0.25 mg per mouse had essentially identical antitumor activity (Supplementary Table S2).

Rapamycin, CP-751,871, or the combination had low or intermediate antitumor activity against ES-1, ES-7, or EW-8 xenografts (Supplementary Table S3). Of note, the combination of rapamycin and CP-751,871 induced complete regressions (CR) of EW-5 xenografts (18 of 18 CRs; Supplementary Table S2). Kaplan-Meier EFS estimates and tumor growth curves for the EWS models are shown in Fig. 2. Against the OS models, CP-751,871 induced regressions of OS-1, and significantly retarded growth of OS-9 but was less effective against OS-2 or OS-17 xenografts (Supplementary Table S2; Fig. 2*B*). Rapamycin was most active against OS-2 and OS-17 xenografts. However, the combination induced CR in all but OS-17 tumors where it significantly inhibited growth over the 12-week period of observation.

Although rapamycin significantly inhibited growth of Rh18 RMS xenografts, it caused few regressions (2 of 10 CR), whereas the combination induced CR in 9 of 10 mice (Supplementary Table S2). The combination had essentially additive activity against Rh30 tumors, but induced no regressions, consistent with the data of Cao and colleagues (40).

Pharmacodynamic and morphologic studies. Downstream substrates for IGF-1R [pAKT(Ser473)] and mTORC1 [pS6(Ser235/6)] were examined in tumor tissues 25 and 169 hours after initiating therapy with CP-751,871, rapamycin, or the combination. Tumors were harvested 1 hour after the final dose of rapamycin.

EWS xenografts. Three tumors (ES-1, ES-7, and EW-8) showed progressive growth, and were considered as failing each therapy (Fig. 3*A*). Three other EWS models showed some sensitivity to rapamycin (ES-2 and ES-8) or both agents (EW-5; Fig. 3*B*). For example, in the ES-1 model, neither single agent significantly retarded growth, whereas the combination was somewhat more effective over the first 7 days of treatment (mean 44% growth inhibition). For all ES tumors, failure to respond to CP-751,871 was characterized by a failure to down-regulate IGF-1R, to suppress pAKT levels, or to completely suppress pS6. In contrast, EW-5 xenografts were growth inhibited ($\sim$94% by day 7), and showed dramatic down-regulation of IGF-1R, decreased pAKT, and diminished pS6 over this time period.

Synergistic antitumor activity of CP-751,871 combined with rapamycin in EW-5 was not paralleled by a significant change in the pharmacodynamic markers over those seen with each agent individually. Morphologic examination of EW-5 tumors at 169 hours showed a dramatic loss of tumor cells and subtotal replacement of the tumor implantation bed by adipose tissue. This was due to both cessation of proliferation ($\sim$10-fold decrease of percentage of Ki67-positive tumor cells), and induction of apoptosis (as confirmed by TUNEL assay) in combination-treated tumors (Fig. 3*C*).

Osteosarcoma xenografts. Compared with either single agent, the combination of CP-751,871 with rapamycin extended EFS in all OS tumor models and increased the fraction of mice that were in CR at week 12 (Supplementary Table S2). CP-751,871 alone induced regressions of some OS-1 xenografts and retarded the growth of OS-2 and OS-9 tumors. CP751,871 caused down-regulation of IGF-1R in OS-1 and OS-2 models, but suppressed p-AKT in OS-1, OS-2, and OS-9 tumors, despite failing to down-regulate IGF-1R in the latter model (Fig. 4). Antibody treatment effectively suppressed rapamycin-induced hyperphosphorylation of AKT (Ser473) in all OS models except OS-17.

Similar pharmacodynamic changes in OS-1 tumors were obtained with the combined treatment with rapamycin and CP-751,871, although the combination was more efficacious with 11 of 13 mice being in CR compared with 2 of 20 CP-751,871–treated mice at the end of the observation period (12 weeks). Similar pharmacodynamic effects were detected in OS-2 tumors treated with CP-751,871, although these xenografts progressed during the first 7 days of treatment. OS-2 tumors treated with the combination of CP-751,871 and rapamycin regressed, but changes in pharmacodynamic parameters did not distinguish between the effects of CP-751,871, rapamycin, or the combination treatment (Fig. 4). However, by immunohistochemical staining, the combination of CP-751,871 and rapamycin had greater than additive activity in reducing proliferation in OS-9 xenografts, as determined by Ki-67 staining, (Supplementary Fig. S1).

Therapy-induced changes in tumor-derived VEGF. As shown in Fig. 1, rapamycin and CP-751,871 each reduced secretion of VEGF by EWS cells *in vitro*. To determine whether changes of tumor-derived VEGF correlated with the antitumor effect of each agent, alone, or in combination, levels were determined by a human-specific VEGF ELISA.

EWS xenografts. Drug-induced changes in VEGF are shown for EWS (Fig. 5*A*). In contrast to the relatively modest effect measured *in vitro*, CP-751,871 significantly and markedly suppressed VEGF levels within 25 hours in ES-1, EW-5, and EW-8 models ($P < 0.002$). Of note, levels of VEGF in control tumors had increased by day 7, probably reflecting their increase in mass and increased hypoxic regions within these larger tumors. On day 7 of treatment, levels of VEGF were significantly decreased from controls in ES-1, EW-5,

Downloaded from http://aacrjournals.org/cancerres/article-pdf/69/19/7662/2616060/7662.pdf by guest on 05 October 2022

and EW-8 xenograft models, with extremely low levels (<10 ng/mL) detected in EW-5 tumors. In contrast to CP751,871, rapamycin treatment had a small effect on decreasing VEGF at 25 hours reaching significance in only ES-2, EW-5, and EW-8 xenografts ($P < 0.05$). On day 7, treatment with rapamycin only decreased VEGF significantly in ES-8 tumors, whereas rapamycin stimulated tumor-associated VEGF in ES-1 at both examined time points.

Osteosarcoma xenografts. The basal level of tumor-associated VEGF was low in OS-1, OS-2, and OS-9 tumors, being 31, 0.33, and 51 ng/mg protein, respectively, whereas the basal level of VEGF associated with OS-17 xenografts was 251 ng/mg protein. CP751,871 treatment significantly decreased VEGF levels in OS-1 and OS-9 xenografts ($P < 0.002$), whereas VEGF was not detected in OS-2 tumors at 25 hours. In contrast, CP751,871 increased VEGF associated with OS-17 tumors ($P = 0.05$) at this time point. At 169 hours of treatment, CP751,871 completely suppressed VEGF in OS-1, OS-2, and OS-9 xenografts, whereas the levels in OS-17 were significantly reduced from that in control tumors ($P < 0.0001$); Fig. 5*B*. Rapamycin treatment did not significantly decrease tumor-associated VEGF levels at 25 or 169 hours in any OS tumor line. However, at 169 hours, rapamycin treatment was associated with significantly elevated levels of VEGF in OS-1 ($P = 0.036$) and OS-17 ($P = 0.0001$) xenografts. Treatment with the combination of CP751,871 and rapamycin significantly decreased tumor-associated VEGF at both time points examined in all models ($P < 0.0001$) except OS-17 where the decrease did not reach statistical significance ($P = 0.0503$) at the 25-hour determination.

CP-751,871 rapidly suppresses VEGF transcription. To determine the mechanism by which CP-751,871 suppressed tumor-derived VEGF, RNA was extracted from control or CP-751,871–treated tumors and VEGF transcripts were determined by quantitative RT-PCR as described in Materials and Methods. Tumors from the 25-hour time point were used, rather than 169 hours into treatment, as marked tumor regression had occurred at the latter time. Three CP-751,871 nonresponding tumors (ES-7, ES-8, and OS-17) and two responding tumors (EW-5 and OS-1) were analyzed. As shown in Fig. 6, decreased VEGF transcripts determined by RT-PCR paralleled decreased levels of VEGF determined by ELISA 25 hours after the first dose of CP-751,871.

Downloaded from http://aacrjournals.org/cancerres/article-pdf/69/19/7662/2616060/7662.pdf by guest on 05 October 2022

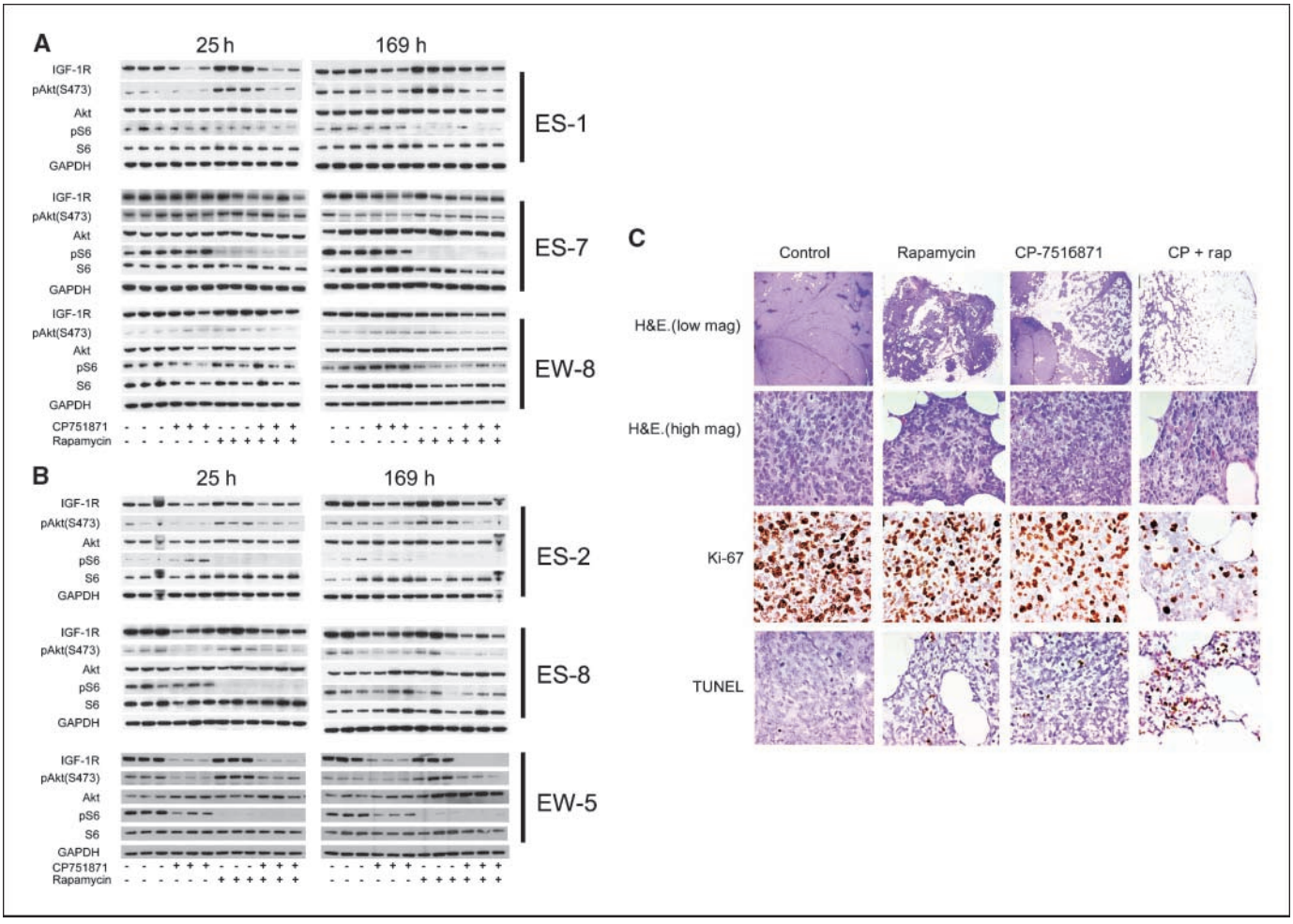

Figure 3. Pharmacodynamic changes in EWS xenografts associated with treatment regimens. Mice received CP-751,871 (0.5 mg/mouse) twice weekly, rapamycin daily 5 d per week, or the combination. Tumors were harvested 1 h after the last dose of rapamycin, and snap-frozen in liquid N_2. Extracts were prepared from tumors and processed as described in Materials and Methods. For each condition (control, CP-751,871, rapamycin, or the combination), three independent tumors were used at each time point. *A,* nonresponsive EWS xenografts. *B,* EWS xenografts responding to at least one agent or the combination. *C,* histology and immunohistochemistry of control EW-5 tumors or after 169 h of treatment with rapamycin, CP-751,871, or the combination (*CP + rap*). Tumor sections were stained for Ki-67, a marker for proliferation, and apoptosis (TUNEL).

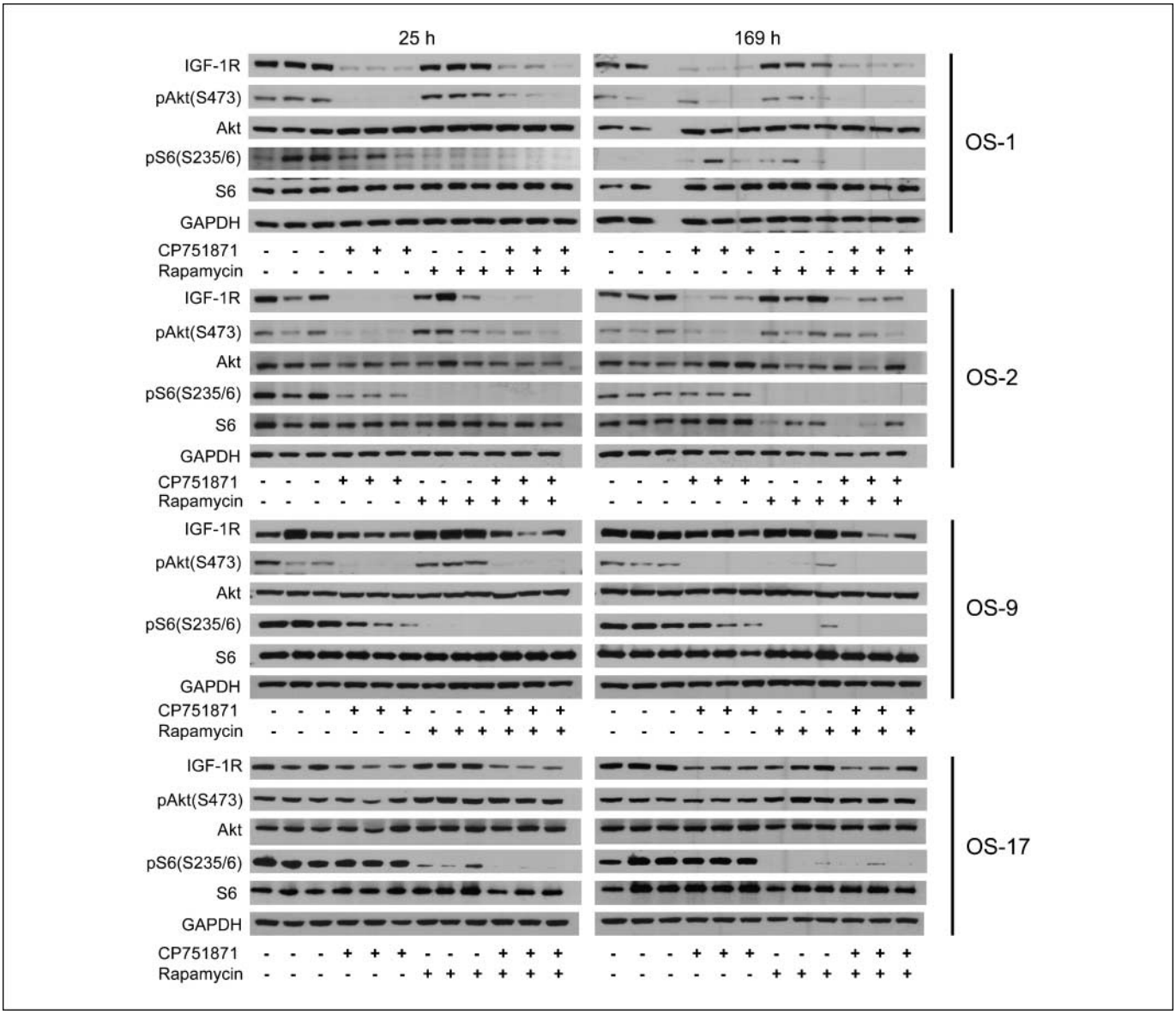

Figure 4. Pharmacodynamic changes in OS xenografts associated with treatment regimens. Mice received CP-751,871 (0.5 mg/mouse) twice weekly, rapamycin daily 5 d per week, or the combination. Tumors were harvested 1 h after rapamycin administration, and snap-frozen in liquid N_2. Extracts were prepared from tumor powders and processed as described in Materials and Methods. For each condition (control, CP-751,871, rapamycin, or the combination), three independent tumors were used at each time point.

Discussion

Panels of childhood cancer xenografts (32) accurately recapitulate the expression profiles of their respective clinical histotypes (41, 42). Reference to this Pediatric Preclinical Testing Program Affymetrix database[4] revealed that expression of IGF-1R was upregulated in most EWS, OS, and RMS models, as was expression of either IGF-1 or IGF-2. Relative secretion of IGF-1 or IGF-2 was confirmed in cell lines using an ELISA, showing that EWS lines secrete more IGF-1, whereas RMS secrete far higher levels of IGF-2 than IGF-1 (data not shown). However, inhibition of proliferation for EWS or RMS (data not shown) cells *in vitro* was relatively modest when cells were exposed to CP-751,871. Similar results were reported for another IGF-1R–targeting antibody, SCH717454 (43). As reported previously (36, 38, 39), rapamycin-induced phosphorylation of AKT(Ser473) in the sarcoma cell lines was studied. In part, increased activation of AKT is a consequence of IRS-1 stabilization when mTORC1 signaling is attenuated. However, rapamycin also increased phosphorylation of the IGF-1R and increased secretion of IGF-1 in EWS cell lines. CP-751,871 blocked IGF-mediated rescue and enhanced rapamycin-induced apoptosis in all EWS and RMS cell lines under serum-free conditions. Further, inhibition of two points in this signaling cascade was found to be additive in suppressing secretion of VEGF (36). Consistent with these observations, combining rapamycin and CP-751,871 decreased secretion of VEGF in most EWS cell lines.

The antitumor activity of rapamycin, CP-751,871 and the combination of agents was tested against 12 sarcoma models

[4] http://pptp.stjude.org/affyData.php?dir=/doc/affyData/Expression/CEL

Downloaded from http://aacrjournals.org/cancerres/article-pdf/69/19/7662/2616060/7662.pdf by guest on 05 October 2022

using response criteria developed for the Pediatric Preclinical Testing Program (supplemental response definitions). As a single agent CP-751,871 exhibited intermediate activity using EFS [EFS(T/C) $\geq$ 2.0] in EW-5, OS-1, and OS-9 xenografts only. For EWS xenografts, the highest level of IGF-1R was in the most sensitive line (EW-5; Supplementary Fig. S2); however, there was no strict correlation between IGF-1R levels and CP-751,871–induced growth inhibition. CP-751,871 induced similar growth inhibition against Rh30, Rh18, and OS-17 xenografts [EFS(T/C), 1.4–1.6] that have quite different receptor levels. Hence, the correlation reported for sarcoma cell lines determined *in vitro* (40) seems less robust *in vivo*.

The combination of CP-751,871 with rapamycin was supra-additive against EW-5 and OS-9 models. In addition, for OS-1 OS, the combination induced 10 of 10 CRs, whereas the CP-751,871 alone induced 4 of 9 CRs, and in OS-2, the combination resulted in partial regression or CR for all tumors compared with progressive disease in the single-agent groups. CP-751,871 significantly inhibited Rh18 xenografts [EFS(T/C), 1.6; P = 0.0015]; however, although the combination inhibited growth similar to that of single agent rapamycin [EFS(T/C) > 15.5], it induced 9 of 10 CRs compared with only 2 of 10 for rapamycin alone. For Rh30 xenografts, the combination EFS(T/C) was essentially additive for the two individual agents, with no tumor regressions. Using objective response criteria, combining CP-751,871 with rapamycin clearly increased the objective response rate in EW-5, OS-1, OS-2, OS-9, and Rh18 xenograft models compared with either monotherapy.

Identifying pharmacodynamic markers of tumor response to rapalogs has proven to be difficult in clinical trials (44). Specifically, markers of decreased mTORC1 signaling tend to be inhibited irrespective of tumor response. We attempted to identify pharmacodynamic markers in tumor tissue that "tracked" with the antitumor activity of both single agents and the combination. The effect of CP-751,871 on down-regulating IGF-1R was highly tumor specific. Rapid loss of receptor was found for EW-5, OS-1, and OS-2 xenografts, whereas IGF-1R was not diminished in many other tumors (ES-7, EW-8, ES-8, and OS-9). However, immunoblotting, as used here, does not distinguish between membrane-associated receptor or internalized receptor that has not been degraded. Tumors where the combination of CP-751,871 and rapamycin was highly effective at causing tumor regression (OS-1,

Downloaded from http://aacrjournals.org/cancerres/article-pdf/69/19/7662/2616060/7662.pdf by guest on 05 October 2022

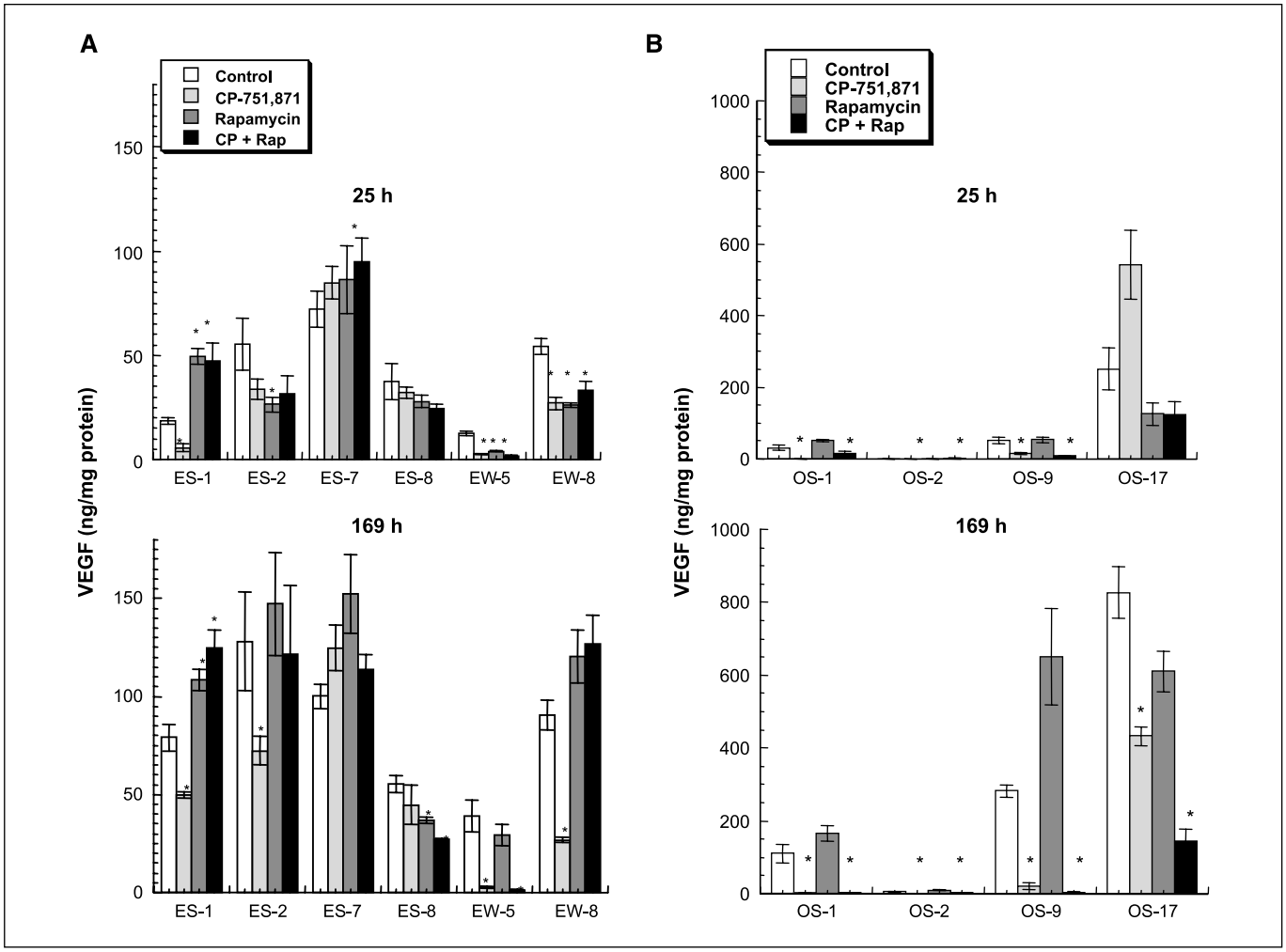

Figure 5. VEGF levels in control and treated tumor xenografts. Mice received CP-751,871 (0.5 mg/mouse) twice weekly, rapamycin daily 5 d per week, or the combination. Tumors were harvested 1 h after the last dose of rapamycin, and snap-frozen in liquid N_2. Extracts were prepared from tumors and VEGF determined by a human-specific ELISA as described in Materials and Methods. For each condition (control, CP-751,871, rapamycin, or the combination), six to nine independent determinations were used at each time point. *, significantly different from controls (P < 0.05). *A,* EWS xenografts. *B,* OS xenografts.

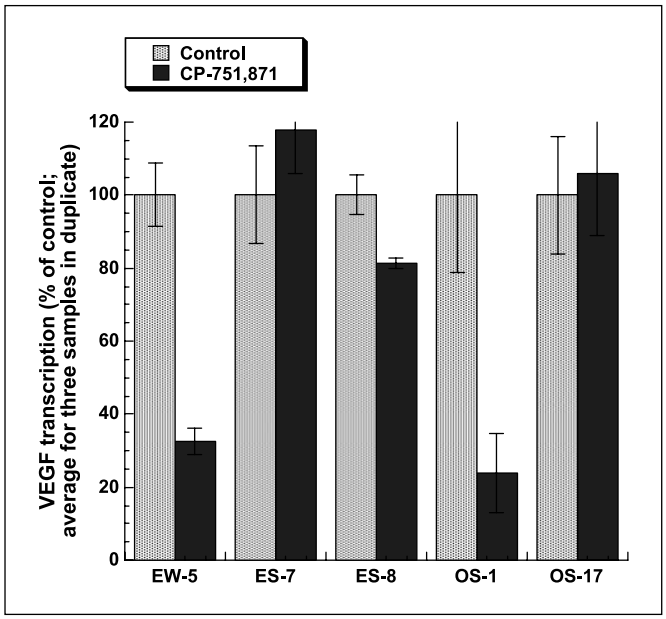

Figure 6. VEGF gene expression in control and CP-751,871–treated tumor xenografts. Total RNA was extracted from the tumors 25 h after administration of CP-751871, reverse transcribed to cDNA, and further quantified by real-time RT-PCR as described in Materials and Methods. The quantity of cDNA in each reaction was normalized to GAPDH and calculated as a ratio of sample cDNA to GAPDH cDNA. Each column represents an average value for duplicate determinations from three independent tumors (±SEM). Sample values were plotted in the histogram as per cent of control tumors (untreated). Control levels being set to 100% for each tumor line.

OS-2, OS-9, EW-5, and Rh18) showed complete suppression of pS6 and marked reduction in IGF-1R levels at 169 hours. The role for pAKT(Ser473) is less clear, as phosphorylation at 169 hours had returned to control levels in EW-5 and OS-2 tumors, despite these xenografts regressing on combination treatment. Rapamycin induced hyperphosphorylation of AKT(Ser473) at 25 and 169 hours in most tumor models, suggesting that irrespective of continued treatment with rapamycin that blocked mTORC1 signaling, mTORC2 signaling remained intact during this period. Notably, CP-751,871 blocked completely (ES-8, EW-5, OS-1, and OS-9) or partially (OS-2 and OS-17) rapamycin-induced hyperphosphorylation of AKT(Ser473). However, CP-751,871 also partially blocked rapamycin-induced pAKT(Ser473) in the ES-1 xenograft line that was poorly responsive to any therapy [EFS(T/C) < 2.0]. Combination treatment also significantly decreased Ki67 staining in EW-5 and OS-9 xenografts, but increased the frequency of TUNEL-positive cells in EW-5 only.

Inhibition of mTORC1 signaling may have direct effect on cell proliferation and survival, or an indirect effect *via* inhibition of HIF-1α, thus reducing tumor-elicited VEGF. Conversely, phosphoinositide 3-kinase/AKT signaling can induce tumor angiogenesis by regulating VEGF. This regulation occurs at both the mRNA and protein levels, and its regulation of VEGF mRNA seems to occur by both HIF-1α–dependent and HIF-1α–independent mechanisms (45). Rapamycin may also exert direct effect on vascular endothelial cells, or vascular smooth muscle cells (46, 47). Guba and colleagues (48) concluded that the antitumor activity of rapamycin was due to its antiangiogenic activity as rapamycin decreased production of VEGF and markedly inhibited response of vascular endothelial cells to stimulation by VEGF. In our study, the pharmacodynamic markers for supra-additive activity for the combination were significant down-regulation of IGF-1R and complete suppression of phospho-S6 for up to 169 hours. Most notably, within 25 hours of administration, CP-751,871 induced a very marked decrease in VEGF in EW-5, OS-1, OS-2, and OS-9 xenografts, and suppression of VEGF was maintained at 169 hours. Consistent with decreased VEGF in tumor tissue, levels of VEGF transcripts were reduced only in tumors where CP-751,871 suppressed levels of VEGF within 25 hours of treatment. In contrast to treatment with CP-751,871, rapamycin treatment stimulated tumor-derived VEGF levels above control tumor levels at 25 hours (ES-1) or 169 hours of treatment (ES-1, ES-7, and OS-9), and partly antagonized the suppression of VEGF by CP-751,871 in ES-1, EW-8, and Rh30 xenografts. Importantly, suppression of tumor-derived VEGF correlated with marked down-regulation of IGF-1R and decreased pAKT induced by CP-751,871. Of note, only in these tumors (EW-5, OS-1, OS-2, and OS-9) was there a marked increase in the frequency of objective tumor responses and maintained CRs when CP-751,871 was combined with rapamycin.

Our results suggests that under conditions of tumor growth *in vivo*, IGF-1R signaling significantly regulates VEGF production despite continued evidence of mTORC1 activity (as shown by maintained phospho-S6). Synergy of the rapamycin-CP-751,871 combination occurred in tumors with low endogenous VEGF (<13 ng/mg protein; EW-5, Rh18, and OS-2) or where CP-751,871 dramatically decreased VEGF (OS-1 and OS-9). In contrast to CP-751,871, rapamycin had less effect on tumor-derived VEGF, and partially antagonized CP-751,871, despite the combination demonstrating synergistic antitumor activity. Thus, suppression of tumor-derived VEGF is only part of the mechanism, as CP-751,871 alone did not cause tumor regressions, except in OS-1 xenografts. This suggests a model in which one agent (CP-751,871) predominantly suppresses the ability of tumors to synthesize VEGF, which in itself is insufficient to completely suppress tumor growth, whereas the other agent (rapamycin) blocks the response to VEGF in cells of the vascular compartment. This model predicts that tumors with the lowest basal levels of VEGF would be the most sensitive to rapamycin. Indeed, the two most rapamycin-sensitive xenograft lines, Rh18 and OS-2 [EFS (T/C) >15.5 and >6.6, respectively], had the lowest basal levels of VEGF, although OS-17 tumors were somewhat rapamycin-sensitive [EFS (T/C) = 5.5] but had extremely high VEGF levels. Based on these data, it seems essential to reduce tumor levels of VEGF to a very low level through inhibiting IGF-1R for rapamycin to effectively synergize. If this model is correct, IGF-1R blockade (to reduce VEGF levels) in combination with small molecule inhibitor of VEGF receptors or bevacizumab, may also be an effective strategy for treatment of these sarcomas.

Disclosure of Potential Conflicts of Interest

P.J. Houghton: commercial research grant and consultant/advisory board. The other authors disclosed no potential conflicts of interest.

Acknowledgments

Received 5/11/09; revised 7/16/09; accepted 7/28/09; published OnlineFirst 9/29/09.

Grant support: USPHS grants CA23099, CA77776, and CA21675 (Cancer Center Support grant), and by American, Lebanese, Syrian Associated Charities.

The costs of publication of this article were defrayed in part by the payment of page charges. This article must therefore be hereby marked *advertisement* in accordance with 18 U.S.C. Section 1734 solely to indicate this fact.

We thank Claire Boltz, Shea Mercer, Jeri Carol Crumpton, Doris Phelps, Dorothy Bush, and Charlene Henry for excellent technical assistance.

Downloaded from http://aacrjournals.org/cancerres/article-pdf/69/19/7662/2616060/7662.pdf by guest on 05 October 2022

References

1. Ayalon D, Glaser T, Werner H. Transcriptional regulation of IGF-I receptor gene expression by the PAX3-FKHR oncoprotein. Growth Horm IGF Res 2001; 11:289–97.
2. Fukuzawa R, Umezawa A, Ochi K, Urano F, Ikeda H, Hata J. High frequency of inactivation of the imprinted H19 gene in "sporadic" hepatoblastoma. Int J Cancer 1999;82:490–7.
3. Minniti CP, Tsokos M, Newton WA, Jr., Helman LJ. Specific expression of insulin-like growth factor-II in rhabdomyosarcoma tumor cells. Am J Clin Pathol 1994; 101:198–203.
4. Scotlandi K, Benini S, Nanni P, et al. Blockage of insulin-like growth factor-I receptor inhibits the growth of Ewing's sarcoma in athymic mice. Cancer Res 1998;58: 4127–31.
5. Scotlandi K, Benini S, Sarti M, et al. Insulin-like growth factor I receptor-mediated circuit in Ewing's sarcoma/peripheral neuroectodermal tumor: a possible therapeutic target. Cancer Res 1996;56:4570–4.
6. Prieur A, Tirode F, Cohen P, Delattre O. EWS/FLI-1 silencing and gene profiling of Ewing cells reveal downstream oncogenic pathways and a crucial role for repression of insulin-like growth factor binding protein 3. Mol Cell Biol 2004;24:7275–83.
7. Pollak M, Richard M. Suramin blockade of insulinlike growth factor I-stimulated proliferation of human osteosarcoma cells. J Natl Cancer Inst 1990;82:1349–52.
8. Bostedt KT, Schmid C, Ghirlanda-Keller C, Olie R, Winterhalter KH, Zapf J. Insulin-like growth factor (IGF) I down-regulates type 1 IGF receptor (IGF 1R) and reduces the IGF I response in A549 non-small-cell lung cancer and Saos-2/B-10 osteoblastic osteosarcoma cells. Exp Cell Res 2001;271:368–77.
9. MacEwen EG, Pastor J, Kutzke J, et al. IGF-1 receptor contributes to the malignant phenotype in human and canine osteosarcoma. J Cell Biochem 2004;92:77–91.
10. El-Badry OM, Helman LJ, Chatten J, Steinberg SM, Evans AE, Israel MA. Insulin-like growth factor II-mediated proliferation of human neuroblastoma. J Clin Invest 1991;87:648–57.
11. Weber A, Huesken C, Bergmann E, Kiess W, Christiansen NM, Christiansen H. Coexpression of insulin receptor-related receptor and insulin-like growth factor 1 receptor correlates with enhanced apoptosis and dedifferentiation in human neuroblastomas. Clin Cancer Res 2003;9:5683–92.
12. Sandberg AC, Engberg C, Lake M, von Holst H, Sara VR. The expression of insulin-like growth factor I and insulin-like growth factor II genes in the human fetal and adult brain and in glioma. Neurosci Lett 1988;93:114–9.
13. Resnicoff M, Li W, Basak S, Herlyn D, Baserga R, Rubin R. Inhibition of rat C6 glioblastoma tumor growth by expression of insulin-like growth factor I receptor antisense mRNA. Cancer Immunol Immunother 1996;42: 64–8.
14. Antoniades HN, Galanopoulos T, Neville-Golden J, Maxwell M. Expression of insulin-like growth factors I and II and their receptor mRNAs in primary human astrocytomas and meningiomas; *in vivo* studies using *in situ* hybridization and immunocytochemistry. Int J Cancer 1992;50:215–22.
15. Del Valle L, Enam S, Lassak A, et al. Insulin-like growth factor I receptor activity in human medulloblastomas. Clin Cancer Res 2002;8:1822–30.
16. Hirschfeld S, Helman L. Diverse roles of insulin-like growth factors in pediatric solid tumors. *In vivo* (Athens, Greece) 1994;8:81–90.
17. Scharf JG, Braulke T. The role of the IGF axis in hepatocarcinogenesis. Horm Metab Res 2003;35:685–93.
18. Braczkowski R, Schally AV, Plonowski A, et al. Inhibition of proliferation in human MNNG/HOS osteosarcoma and SK-ES-1 Ewing sarcoma cell lines *in vitro* and *in vivo* by antagonists of growth hormone-releasing hormone: effects on insulin-like growth factor II. Cancer 2002;95:1735–45.
19. Cohen BD, Baker DA, Soderstrom C, et al. Combination therapy enhances the inhibition of tumor growth with the fully human anti-type 1 insulin-like growth factor receptor monoclonal antibody CP-751,871. Clin Cancer Res 2005;11:2063–73.
20. Wang Y, Hailey J, Williams D, et al. Inhibition of insulin-like growth factor-I receptor (IGF-IR) signaling and tumor cell growth by a fully human neutralizing anti-IGF-IR antibody. Mol Cancer Ther 2005;4:1214–21.
21. Guerreiro AS, Boller D, Doepfner KT, Arcaro A. IGF-IR: potential role in antitumor agents. Drug News Perspect 2006;19:261–72.
22. Kurmasheva RT, Houghton PJ. IGF-I mediated survival pathways in normal and malignant cells. Biochim Biophys Acta 2006;1766:1–22.
23. Sachdev D, Yee D. Inhibitors of insulin-like growth factor signaling: a therapeutic approach for breast cancer. J Mammary Gland Biol Neoplasia 2006;11:27–39.
24. Sachdev D, Yee D. Disrupting insulin-like growth factor signaling as a potential cancer therapy. Mol Cancer Ther 2007;6:1–12.
25. Sachdev D, Li SL, Hartell JS, Fujita-Yamaguchi Y, Miller JS, Yee D. A chimeric humanized single-chain antibody against the type I insulin-like growth factor (IGF) receptor renders breast cancer cells refractory to the mitogenic effects of IGF-I. Cancer Res 2003;63: 627–35.
26. Goetsch L, Gonzalez A, Leger O, et al. A recombinant humanized anti-insulin-like growth factor receptor type I antibody (h7C10) enhances the antitumor activity of vinorelbine and anti-epidermal growth factor receptor therapy against human cancer xenografts. Int J Cancer 2005;113:316–28.
27. Wullschleger S, Loewith R, Hall MN. TOR signaling in growth and metabolism. Cell 2006;124:471–84.
28. Bjornsti MA, Houghton PJ. The TOR pathway: a target for cancer therapy. Nat Rev Cancer 2004;4:335–48.
29. Dilling MB, Dias P, Shapiro DN, Germain GS, Johnson RK, Houghton PJ. Rapamycin selectively inhibits the growth of childhood rhabdomyosarcoma cells through inhibition of signaling via the type I insulin-like growth factor receptor. Cancer Res 1994;54:903–7.
30. Houchens DP, Ovejera AA, Riblet SM, Slagel DE. Human brain tumor xenografts in nude mice as a chemotherapy model. Eur J Cancer Clin Oncol 1983;19: 799–805.
31. Houghton PJ, Morton CL, Kolb EA, et al. Initial testing (stage 1) of the mTOR inhibitor rapamycin by the pediatric preclinical testing program. Pediatr Blood Cancer 2008;50:799–805.
32. Houghton PJ, Morton CL, Tucker C, et al. The pediatric preclinical testing program: description of models and early testing results. Pediatr Blood Cancer 2006;49:928–40.
33. Meyer WH, Houghton JA, Houghton PJ, Webber BL, Douglass EC, Look AT. Development and characterization of pediatric osteosarcoma xenografts. Cancer Res 1990;50:2781–5.
34. Thimmaiah KN, Easton J, Huang S, et al. Insulin-like growth factor I-mediated protection from rapamycin-induced apoptosis is independent of Ras-Erk1-Erk2 and phosphatidylinositol 3′-kinase-Akt signaling pathways. Cancer Res 2003;63:364–74.
35. Dudkin L, Dilling MB, Cheshire PJ, et al. Biochemical correlates of mTOR inhibition by the rapamycin ester CCI-779 and tumor growth inhibition. Clin Cancer Res 2001;7:1758–64.
36. Kurmasheva RT, Harwood FC, Houghton PJ. Differential regulation of vascular endothelial growth factor by Akt and mammalian target of rapamycin inhibitors in cell lines derived from childhood solid tumors. Mol Cancer Ther 2007;6:1620–8.
37. Houghton PJ, Morton CL, Tucker C, et al. The pediatric preclinical testing program: description of models and early testing results. Pediatr Blood Cancer 2007;49:928–40.
38. Shi Y, Yan H, Frost P, Gera J, Lichtenstein A. Mammalian target of rapamycin inhibitors activate the AKT kinase in multiple myeloma cells by up-regulating the insulin-like growth factor receptor/insulin receptor substrate-1/phosphatidylinositol 3-kinase cascade. Mol Cancer Ther 2005;4:1533–40.
39. O'Reilly KE, Rojo F, She QB, et al. mTOR inhibition induces upstream receptor tyrosine kinase signaling and activates Akt. Cancer Res 2006;66:1500–8.
40. Cao L, Yu Y, Darko I, et al. Addiction to elevated insulin-like growth factor i receptor and initial modulation of the AKT pathway define the responsiveness of rhabdomyosarcoma to the targeting antibody. Cancer Res 2008;68:8039–48.
41. Whiteford CC, Bilke S, Greer BT, et al. Credentialing preclinical pediatric xenograft models using gene expression and tissue microarray analysis. Cancer Res 2007;67:32–40.
42. Neale G, Su X, Morton CL, et al. Molecular characterization of the pediatric preclinical testing panel. Clin Cancer Res 2008;14:4572–83.
43. Kolb EA, Gorlick R, Houghton PJ, et al. Initial testing (stage 1) of a monoclonal antibody (SCH 717454) against the IGF-1 receptor by the pediatric preclinical testing program. Pediatr Blood Cancer 2008;50:1190–7.
44. Tabernero J, Rojo F, Calvo E, et al. Dose- and schedule-dependent inhibition of the mammalian target of rapamycin pathway with everolimus: a phase I tumor pharmacodynamic study in patients with advanced solid tumors. J Clin Oncol 2008;26:1603–10.
45. Arsham AM, Plas DR, Thompson CB, Simon MC. Akt and hypoxia-inducible factor-1 independently enhance tumor growth and angiogenesis. Cancer Res 2004;64: 3500–7.
46. Humar R, Kiefer FN, Berns H, Resink TJ, Battegay EJ. Hypoxia enhances vascular cell proliferation and angiogenesis *in vitro* via rapamycin (mTOR)-dependent signaling. FASEB J 2002;16:771–80.
47. Majumder PK, Febbo PG, Bikoff R, et al. mTOR inhibition reverses Akt-dependent prostate intraepithelial neoplasia through regulation of apoptotic and HIF-1-dependent pathways. Nat Med 2004;10: 594–601.
48. Guba M, von Breitenbuch P, Steinbauer M, et al. Rapamycin inhibits primary and metastatic tumor growth by antiangiogenesis: involvement of vascular endothelial growth factor. Nat Med 2002;8:128–35.

Downloaded from http://aacrjournals.org/cancerres/article-pdf/69/19/7662/2616060/7662.pdf by guest on 05 October 2022